Acta Mechanica Sinica (2012) 28(5):1374–1381
DOI 10.1007/s10409-012-0077-8

RESEARCH PAPER

Tensionless contact of a finite circular plate

Yin Zhang · Kevin D. Murphy

Received: 24 November 2011 / Revised: 9 February 2012 / Accepted: 27 February 2012

Abstract A general formulation is developed for the contact behavior of a finite circular plate with a tensionless elastic foundation. The gap distance between the plate and elastic foundation is incorporated as an important parameter. Unlike the previous models with zero gap distance and large/infinite plate radius, which assumes the lift-off/separation of a flexural plate from its supporting elastic foundation, this study shows that lift-off may not occur. The results show how the contact area varies with the plate radius, boundary conditions and gap distance. When the plate radius becomes large enough and the gap distance is reduced to zero, the converged contact radius close to the previous ones is obtained.

Keywords Tensionless contact · Elastic foundation · Plate · Lift-off

1 Introduction

The separating tendency of a laterally loaded plate from its supports was noticed more than fifty years ago [1]. The bending of flexural structures such as beam and plate under a normal load induces the out-of-plane displacement, which can lead to the lift-off/separation of structures from their supports. The contact problem of a flexural structure is called differently as the receding contact [2], unbonded contact [3, 4], tensionless contact [5–11] and unilateral contact [12, 13]. Despite their different names they all emphasize one essential thing: bending and lift-off of flexural structure. The name of receding contact emphasizes that the contact area under loading is smaller than the unloaded one because of lift-off. The name of unbonded contact emphasizes that the flexural structure is allowed to lift-off/separate from its support. The name of tensionless contact emphasizes that in a non-adhesive contact, tensile stress can not be transmitted to the lift-off parts of structure. The names of tensionless contact and unilateral contact both emphasize that only compressive stress exists in the contact area. The bending and lift-off of flexural structures introduce the localized effect (concentration of stress and strain in a given area), which can have significant impact on the nanoindentation test of one dimensional (1D) nanostructures, such as nanobelt [14] and nanowire [15]. Besides its marvelous electric properties [16], graphene together with other 2D materials of one or a few atomic layers also demonstrates extraordinary friction properties: friction increases monotonously with the decrease of the layer numbers [17]. The"rigid" contact models such as the Hertz and Johnson–Kendall–Roberts (JKR) models are developed for the contact of two spheres in which the contact zone is extremely small compared with the sizes of spheres and the radii of curvature are thus assumed unchanged [14, 15]. By contrast, the out-of-plane bending deflection (and thus the radius of curvature) of flexural structures changes with the normal load. In microscopic scale, friction force F_{f} is proportional to the contact area, i.e., $F_{\mathrm{f}} = \tau A$ (τ is the constant shear strength for given materials and geometry; A is the contact area) [18]. The tangential force is believed to have no impact on the contact area [19]. The thickness of graphene is extremely small compared with its other dimensions, which makes it very flexural. The out-of-plane deflection due to normal loading, referred to as "puckering", is believed to increase the graphene contact area and thus its friction force [17]. This work presents a study on the tensionless contact of a finite circular plate under a concentrated load, which is the loading case of nanoindentation [14, 15] and normal load exerted by an atomic force microscope (AFM) tip in the friction test [17]. The approach presented here may offer some in-

The project was supported by the National Natural Science Foundation of China (11021262 and 11023001) and Chinese Academy of Sciences (KJCX2-EW-L03).

Y. Zhang (✉)
State Key Laboratory of Nonlinear Mechanics (LNM),
Institute of Mechanics, Chinese Academy of Sciences,
100190 Beijing, China
e-mail: zhangyin@lnm.imech.ac.cn

K. D. Murphy
Department of Mechanical Engineering,
the University of Connecticut, Storrs, CT 06269, USA

sights on how to properly evaluate the contact area between an indenter and a 2D flexural structure such as graphene.

The problem formulation of plate tensionless contact can be either integral [3, 7–9, 20] or differential [4–6, 12, 13]. The substrate is modeled either as an elastic half space [3, 20] or as an elastic foundation [4–9, 12, 13]. The elastic half space model in essence is to solve a Boussinesq problem [21]. In an elastic half space model, the displacement, strain and stress at a point is determined by the elastic deformation all over the area and its formulation can only be integral [3, 20]. The formulation of an elastic foundation model can be either integral [7–9] or differential [4–6, 12, 13]. Compared with the differential formulation, the integral formulation and the iterative algorithm needed to solve the problem are rather lengthy and complex. Weitsman [6] presented a differential formulation of a circular plate on a tensionless foundation. However, Weitsman's matching conditions at the separation points assume the disappearance of displacement, bending moment and shear force [6], which are generally not true [4, 10]. Yang also pointed out that the bending moment at the separation point can not be zero [22]. Physically, Weitsman's model is for an infinitely large plate [6]. The difference between an infinitely long beam and a finite beam in tensionless contact is demonstrated by Zhang and Murphy [10]. In the above tensionless contact models of plate [3, 4, 6–9, 12, 13, 20], the gap distance between the plate and support is zero.

In many micro-electro-mechanical systems (MEMS) structures, there is a nonzero gap distance between the micro-structure and substrate [22–28]. Therefore, it is of a practical use to have a nonzero gap distance incorporated in the model. The previous models mentioned above also explicitly assume the lift-off of plate [3, 4, 6–9, 12, 13, 20]. As shown in this study, there is no lift-off for the plate with a small radius and the whole plate is in contact with substrate. Only when the plate radius reaches some critical value and the plate becomes flexural enough, the plate can lift-off from substrate.

2 Model development

As shown in Fig. 1, a circular plate with a radius of R' is separated from a tensionless elastic foundation by a gap distance of Z_o. The boundary conditions can vary as the free, clamped and simply-supported ones. Z_o can only be zero for a free plate. The coordinate system is also shown in Fig. 1, which is at the center of the undeformed plate. The substrate is modeled as Winkler foundation with the modulus of k; D is the plate flexural rigidity and $D = ET^3/12(1-\nu^2)$ (E,T and ν are the plate Young's modulus, thickness and Poisson's ratio, respectively). The circular plate is subjected to a concentrated load P at its center. The plate separates from the elastic foundation once its displacement is less than Z_o. Otherwise, the plate is in contact with the elastic foundation. The plate displacement of W is divided into the following two parts as shown in Fig. 1.

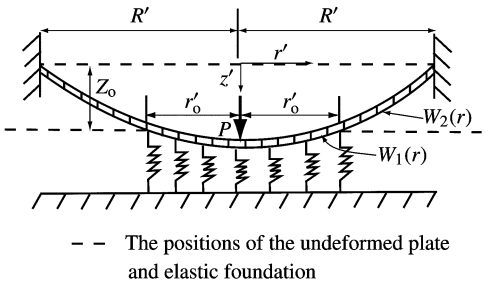

Fig. 1 The schematic diagram of a circular plate under a point load P at the center and the coordinate system. R' is the plate radius, Z_o is the gap distance and r'_o is the contact radius. W_1 and W_2 are the displacements of the contact and lift-off zones, respectively

$$W = \begin{cases} W_1(r'), & \text{contact region,} \\ W_2(r'), & \text{lift-off region.} \end{cases} \tag{1}$$

The governing equation of the contact region is the following [6]

$$D\Delta_{r'}^2\Delta_{r'}^2 W_1 + k(W_1 - Z_o) = \frac{P}{2\pi}\frac{\delta(r')}{r'}, \quad W_1 \geq Z_o, \quad 0 \leq r' \leq r'_o, \tag{2}$$

where r'_o is the unknown plate contact radius as shown in Fig. 1, $\Delta_{r'}^2$ is an operator defined as $\Delta_{r'}^2 = (1/r')(\mathrm{d}/\mathrm{d}r')(r'\mathrm{d}/\mathrm{d}r')$, δ is the Dirac delta function used to model the concentrated load, $k(W_1 - Z_o)$ is the compressive pressure exerted by the elastic foundation due to contact. The governing equation of the lift-off zone is as follows

$$D\Delta_{r'}^2\Delta_{r'}^2 W_2 = 0, \quad W_2 \leq Z_o, \quad r'_o \leq r' \leq R'. \tag{3}$$

The following quantities are introduced to nondimensionalize Eqs. (2) and (3)

$$l^4 = \frac{D}{k}, \quad r = \frac{r'}{l}, \quad w = \frac{W}{l}, \quad z_o = \frac{Z_o}{l}, \quad R = \frac{R'}{l}, \quad r_o = \frac{r'_o}{l}. \tag{4}$$

Equations (2) and (3) are now nondimensionalized as follows

$$\Delta_r^2\Delta_r^2 w_1 + w_1 - z_o = \frac{P}{2\pi Dl^2}\frac{\delta(r)}{r}, \quad w_1 \geq z_o, \quad 0 \leq r \leq r_o, \tag{5}$$

$$\Delta_r^2\Delta_r^2 W_2 = 0, \quad w_2 \leq z_o, \quad r_o \leqslant r \leqslant R. \tag{6}$$

The solutions to Eqs. (5) and (6) are given as follows [6]

$$w_1 = A_1\mathrm{ber}(r) + B_1\mathrm{ber}(r) - 2F_o\mathrm{ber}(r) + z_o, \tag{7}$$

$$w_2 = A_2 r^2 + B_2 \ln r + C_2 r^2 \ln r + D_2, \tag{8}$$

where F_o is a dimensionless quantity defined as $F_o = Pl^2/(4\pi D)$; A_1, B_1, A_2, B_2, C_2 and D_2 are the unknown constants to be determined. ber, bei and kei are the Bessel functions [29], whose forms are given in Appendix I. r^4, r^2, $\ln r$,

$r^2 \ln r$ and constant (D_2) together are all five possible solution function forms for Eq. (6) [30]. However, keep in mind that r^4 is the function form associated with the uniformly distributed load [30]. Because there is no uniformly distributed load, there is no r^4 term in the solution of Eq. (8). There are total seven unknowns (A_1, B_1, A_2, B_2, C_2, D_2 and r_o) to be determined in this formulation.

Here it is heuristic to have a comparison with Weitsman's solution of Eq. (6), which is given as the following for an infinite plate with $R = \infty$ and $z_o = 0$ [6]

$$w_2 = B_2 \ln\left(\frac{r}{r_o}\right). \tag{9}$$

There are only four unknowns in Weitsman's formulation (A_1, B_1, B_2 and r_o). The reason to have the solution form of Eq. (9) is due to the assumption of the vanishing displacement and shear force at the separation point of $r = r_o$ [6]. Here the limitation and drawback of Eq. (9) should be analyzed. Clearly, the solution of Eq. (9), which gives $w_2(r_o) = 0$ can not apply to the case with a nonzero gap distance as shown in Fig. 1. The (dimensionless) shear force in the lift-off zone is given as follows [1]

$$Q_r(r) = \frac{\mathrm{d}^3 w_2}{\mathrm{d}r^3} + \frac{1}{r}\frac{\mathrm{d}^2 w_2}{\mathrm{d}r^2} - \frac{1}{r^2}\frac{\mathrm{d}w_2}{\mathrm{d}r}. \tag{10}$$

By substituting Eq. (9) into Eq. (10), it is readily evident that Q_r of an infinite plate is always zero not only at the separation point but also in the whole lift-off zone of $r_o \leqslant r \leqslant R$. The shear force indeed disappears in the lift-off zone for a finite free plate as shown in Appendix II. However, it is also demonstrated in Appendix II that the shear force in the lift-off zone is not zero for a finite plate with other types of boundary conditions. Therefore, the solution form of Eq. (9) can not apply to the plate with the other types of boundary conditions.

Because the continuity of the displacement and slope, the matching conditions at $r = r_o$ give the following

$$w_1(r_o) = w_2(r_o), \quad \frac{\mathrm{d}w_1(r_o)}{\mathrm{d}r} = \frac{\mathrm{d}w_2(r_o)}{\mathrm{d}r}. \tag{11}$$

The (dimensionless) bending moment is given as follows [1]

$$M_r(r) = -\left[\frac{\mathrm{d}^2 w(r)}{\mathrm{d}r^2} + \frac{\nu}{r}\frac{\mathrm{d}w(r)}{\mathrm{d}r}\right]. \tag{12}$$

In conjunction with the slope continuity condition in Eq. (11), the continuity of bending moment leads to $\mathrm{d}^2 w_1(r_o)/\mathrm{d}r^2 = \mathrm{d}^2 w_2(r_o)/\mathrm{d}r^2$. Similarly, in conjunction with the continuity of both the slope and bending moment, the continuity of shear force concludes $\mathrm{d}^3 w_1(r_o)\mathrm{d}r^3 = \mathrm{d}^3 w_2(r_o)\mathrm{d}r^3$. Therefore, at $r = r_o$, the matching conditions which require the continuity of the bending moment and shear force give the following

$$\frac{\mathrm{d}^2 w_1(r_o)}{\mathrm{d}r^2} = \frac{\mathrm{d}^2 w_2(r_o)}{\mathrm{d}r^2}, \quad \frac{\mathrm{d}^3 w_1(r_o)}{\mathrm{d}r^3} = \frac{\mathrm{d}^3 w_2(r_o)}{\mathrm{d}r^3} \tag{13}$$

The four matching conditions of Eqs. (11) and (13) at $r = r_o$ are the same ones derived by Kerr [4] via a variational approach. The matching conditions are also often referred to as the transversality conditions [4, 26]. The displacement constraint condition at $r = r_o$ is the following [10]

$$w_1(r_o) = z_o. \tag{14}$$

Alternatively, one may use $w_2(r_o) = z_o$. For a free plate, the following boundary conditions of vanishing moment and shear force hold

$$M_r(R) = 0, \quad Q_r(R) = 0. \tag{15}$$

For a clamped plate, the following boundary conditions of vanishing displacement and slope hold

$$w_2(R) = 0, \quad \frac{\mathrm{d}w_2(R)}{\mathrm{d}r} = 0. \tag{16}$$

For a simply-supported plate, the following boundary conditions of vanishing displacement and moment hold

$$w_2(R) = 0, \quad M_r(R) = 0. \tag{17}$$

Therefore, four matching conditions, one constraint condition and two boundary conditions give seven equations in total to solve the seven unknowns of (A_1, B_1, A_2, B_2, C_2, D_2 and r_o). Because r_o is unknown, solving these seven unknowns is a nonlinear problem and Newton–Rhapson method is required [10]. The equation set of A_1, B_1, A_2, B_2, C_2, D_2 and r_o is presented in Appendix III.

3 Results and discussions

3.1 Free circular plate

In this study k and D are taken as 1 for simplicity and comparison reason. For a free circular plate, z_o can only be taken as 0. Figure 2 plots the R versus r_o. The contact radius of r_o in Fig. 2 keeps increasing linearly with increase of the plate radius of R until $R = 2.84$. The slope of the curve is 1. After $R = 2.84$, the contact radius increases with a much smaller slope and the curve is then flattened. The contact radius of r_o converges to 2.665 6 around $R = 40$. Because the boundary condition $M_r(R) = 0$ is applied and $M_r(r)$ as indicated by Eq. (12) is dependent on the plate Poisson's ratio of ν, it is taken as 0.25 in Fig. 2. However, the convergence of r_o is not sensitive to the plate Poisson's ratio of ν at all. The converged contact radius only changes from 2.665 6 of $\nu = 0$ to 2.665 8 of $\nu = 0.5$. It is worth pointing out that the R–r_o curve presented in Fig. 2 is independent of the concentrated load P. The r_o independence of the concentrated load of P is a rather counter-intuitive and important feature of the plate tensionless contact [3, 6, 7, 9]. Because the same problem is computed in Refs. [3, 6, 7, 9], r_o is presented for a comparison in Table 1.

Table 1 r_o of a free plate when $z_o = 0$ and R is infinite or very large

Ref.	r_o
[3]	$2.926\sqrt[3]{\frac{(1-\nu_s)D}{G_s}}\sqrt[4]{\frac{k}{D}}^{*}$
[6]	2.85
[7]	2.76
[9]	2.72
Present study	2.665 6 – 2.665 8

* ν_s and G_s are the Poisson's ratio and shear modulus of the substrate modeled as an elastic half space [3], respectively. The $\sqrt[4]{k/D}$term is due to the nondimensionalization scheme of Eq. (4), which is also shared by Refs. [6, 7, 9].

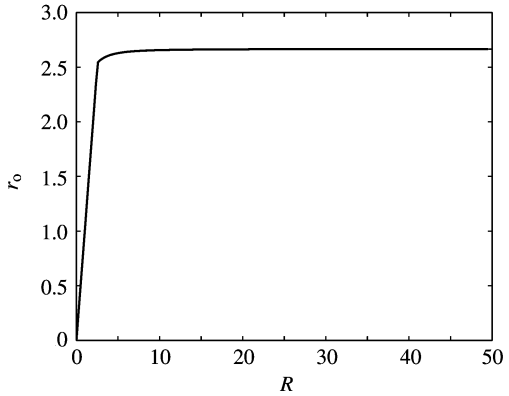

Fig. 2 R–r_o relation for a free circular plate with $z_o = 0$

In the previous models, the plate radius is either infinite [3, 6] or very large compared with the contact radius of r_o [7, 9]. The effect of R on lift-off is thus not presented in the previous studies [3, 6, 7, 9]. Figure 2 is to present such study and shows the R–r_o relation of a free plate with zero gap distance. When $z_o = 0$, the contact radius of r_o is independent of load [3, 6, 7, 9] and therefore R is the unique parameter which can influence r_o in a finite free plate. Two questions should be asked for the R–r_o curve presented in Fig. 2: (1) why does the contact radius of r_o increase linearly with the slope of one until $R = 2.84$? and (2) why is the curve flattened/converged after $R = 2.84$? These two questions can be answered by examining the deflections of plate with different values of R.

Figure 3 shows the deflections of the plate with $R = 2$ and $z_o = 0$ under two different P's. The whole plate is in contact with the elastic foundation under these P's and no lift-off occurs: larger load P just pushes the plate deeper into the elastic foundation. Therefore, the contact radius is the plate radius, i.e., $r_o = R$, which is responsible for the slope of one. It is also necessary to have a discussion on the constraint condition of Eq. (14) in this scenario. It is noticed that the displacements in Fig. 3 are all greater than zero and the constraint condition seems violated. In fact, it is not. What happens is that the contact radius of r_o computed at this scenario is larger than the plate radius of R and the constraint condition is still mathematically satisfied. Of course, it is physically impossible to have $r_o > R$. In this scenario, the contact radius is taken as R not r_o. In this scenario, the assumption in Refs. [3, 6, 7, 9] that lift-off always occurs can not be true. Figure 4 shows the deflections of a free plate with $R = 20$ under two different load P's. The plate now lifts-off at the same $r_o = 2.665\,6$ marked by circles for both loads, which, again, demonstrates the independence of r_o on P [3, 6, 7, 9]. The lift-off mechanism is the reason why the curve in Fig. 2 is flattened/converged after $R = 2.84$.

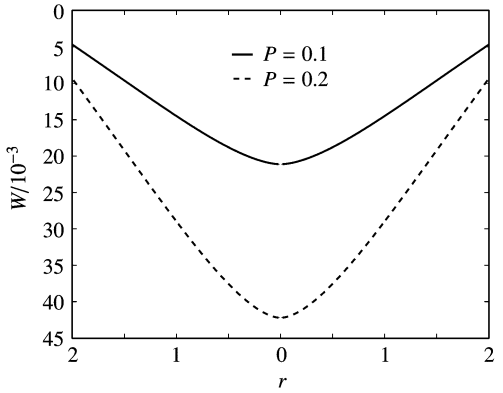

Fig. 3 Deflections of a free plate with $R = 2$ and $z_o = 0$ under $P = 0.1$ and $P = 0.2$. Poisson's ratio of the plate is 0.25

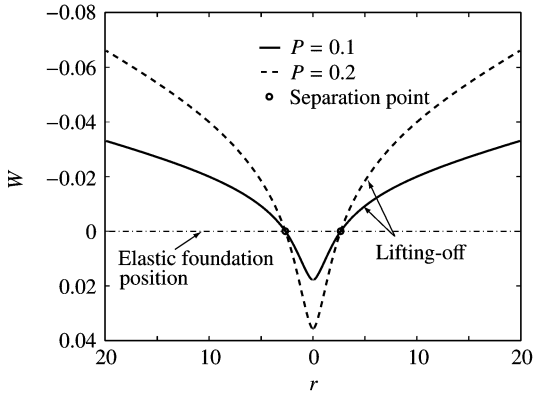

Fig. 4 Deflections of a free plate with $R = 20$ and $z_o = 0$ when $P = 0.1$ and $P = 0.2$. Poisson's ratio of the plate is 0.25

3.2 Clamped circular plate

Compared with a free plate, a clamped plate can have nonzero gap distance of z_o. Figure 5 shows the R–r_o relations with different z_o's at $P = 0.1$. In comparison with Fig. 2, the independence of r_o on P is no longer valid for a clamped plate with a nonzero z_o. When a free-standing clamped circular plate is with a concentrated load P at its center, its displacement is given as follows [1]

$$w(r) = \frac{Pr^2 \ln(r/R)}{8\pi D} + \frac{P(R^2 - r^2)}{16\pi D}. \tag{18}$$

The maximum displacement is the plate center displacement, which gives the following

$$w_{\max} = w(0) = \frac{PR^2}{16\pi D}. \tag{19}$$

Setting the maximum displacement equal to the gap size permits one to determine the plate radius of R at which the contact initiates. Therefore, when $P = 0.1$ and $w_{\max} = z_o = 0.01(D = 1)$, $R = 2.25$; when $P = 0.1$ and $w_{\max} = z_o = 0.1(D = 1)$, $R = 7.12$. This is the reason why the contact radius of $z_o = 0.01$ remains zero until $R = 2.25$ and that of $z_o = 0.1$ until $R = 7.12$ as seen in Fig. 5.

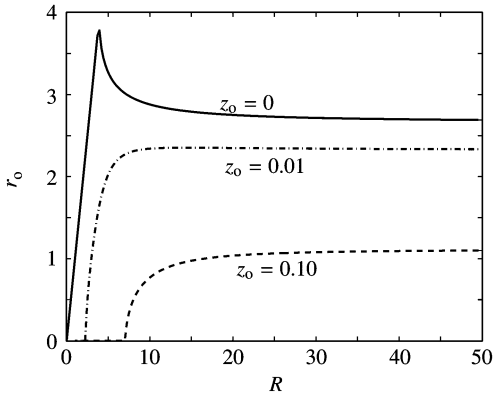

Fig. 5 R–r_o relation for a clamped plate with different z_o's when $P = 0.1$

For the case of $z_o = 0$, Fig. 5 shows that r_o increases linearly with the slope of one until $R = 3.94$, then decreases and finally converges to 2.691. Compared with the converged contact radius of 2.665 6 for a free plate, the plate boundary conditions have a weak influence on r_o of the plate with large R. Again, to explain the r_o–R relation as seen in Fig. 5, we have to examine the deflections of plate with different R's. Figure 6 shows the deflections of a clamped plate with $R = 3$ and $z_o = 0$ under two different P's. Similar to Fig. 3, the whole plate is in contact with the elastic foundation and there is no lift-off; larger load P pushes the plate deeper into the elastic foundation. Figure 7 shows the deflections of the plate with $R = 20$ and $z_o = 0$ under two different concentrated loads. The plate now lifts off at the same $r_o = 2.75$ for two different P's. Again, for a clamped plate, the same fact that the whole plate is in contact with the foundation is responsible for the result that r_o increases with the slope of one when R is relatively small; the lift-off is also the mechanism responsible for the convergence of r_o.

Figure 8 shows the plate radius versus contact radius with different gap distances under a much larger load of $P = 1$. Compared with Fig. 5, the curve with $z_o = 0$ keeps unchanged. Other two curves with finite z_o change dramatically. They come closer to the curve with zero gap distance.

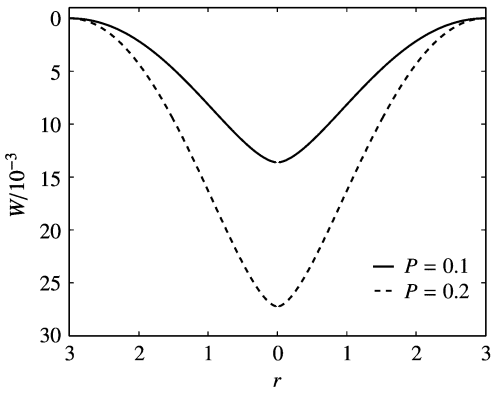

Fig. 6 Deflections of a clamped plate with $R = 3$ and $z_o = 0$ when $P = 0.1$ and $P = 0.2$

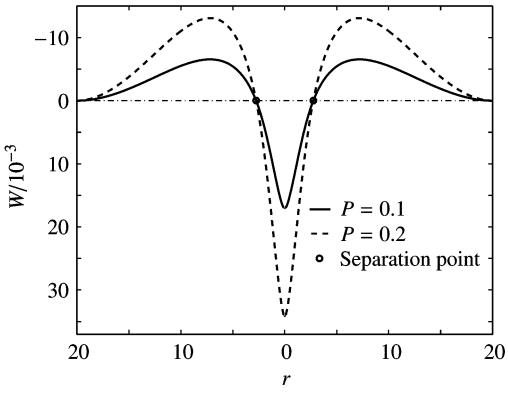

Fig. 7 Deflections of a clamped plate with $R = 20$ and $z_o = 0$ when $P = 0.1$ and $P = 0.2$

The comparison between Figs. 5 and 8 clearly shows the breakdown of the independence of r_o on P for nonzero z_o's. For the same nonzero z_o, a larger load ($P = 1$) in Fig. 8 has larger r_o than that of a smaller load ($P = 0.1$) in Fig. 5. It is also noticed that when the contact is initiated, all these three r_o's start at 0, which physically corresponds to the point contact. With the presence of adhesion, r_o will start with a finite number rather than zero [26, 27]. The model presented here does not incorporate the adhesion effect. Adhesion is a rather weak surface interaction and its effect stands out only when both the structure dimension and mechanical load are small [14]. Adhesion can have significant impact on the indentation [14, 15], friction [17, 18] and stiction [22–25, 27] of micro/nano-scale structures. The study of adhesion effect on the plate contact will be carried out in our future work.

Figures 9 and 10 are both with $R = 20$ and $z_o = 0.1$. Figure 9 shows the deflections of the plate under two relatively small Ps. The contact radius is 1.037 for $P = 0.1$ and 1.462 for $P = 0.2$. Figure 10 shows these deflection shapes of the plate under much larger P's. The contact radius increases to $r_o = 2.349$ for $P = 1$ and $r_o = 2.5$ for $P = 2$. Clearly the deflection shapes in Fig. 10 are very different from those in Fig. 9.

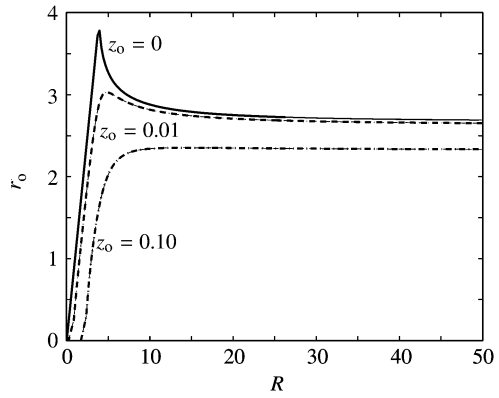

Fig. 8 R–r_o relation for a clamped plate with different z_o's when $P = 1$

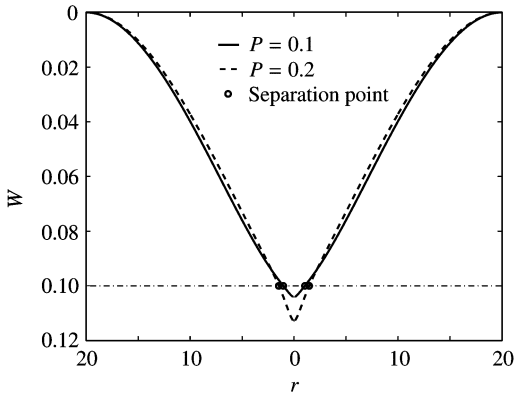

Fig. 9 Deflections of a clamped plate with $R = 20$ and $z_o = 0.1$ under relatively small loads of $P = 0.1$ and $P = 0.2$

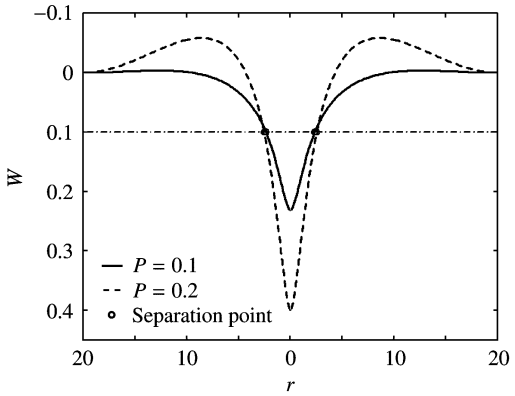

Fig. 10 Deflections of a clamped plate with $R = 20$ and $z_o = 0.1$ under relatively large loads of $P = 1$ and $P = 2$

Figure 11 shows the z_o–r_o relation under two different P's for a clamped plate with $R = 20$, which is a way of showing the r_o dependence on z_o and P. The two curves starts from the same point of (0, 2.75) because at $z_o = 0$ the contact radius of r_o is independent of load P. This is also the only point they share. For the curve with $P = 0.1$, the contact radius becomes zero at $z_o = 0.795\,8$. For the curve with $P = 0.2$, the contact radius r_o becomes zero at $z_o = 2 \times 0.795\,8$. The reason for this is that for $R = 20$ and $P = 0.1$, the maximum plate displacement calculated from Eq. (19) is $0.795\,8$. So if the gap distance z_o is larger than $0.795\,8$, the plate with $R = 20$ has no contact with the elastic foundation under a given load of $P = 0.1$. Also from Eq. (19), w_{max} is linear with load P, that is why for $P = 0.2$ the contact radius r_o becomes zero at $z_o = 2 \times 0.795\,8$.

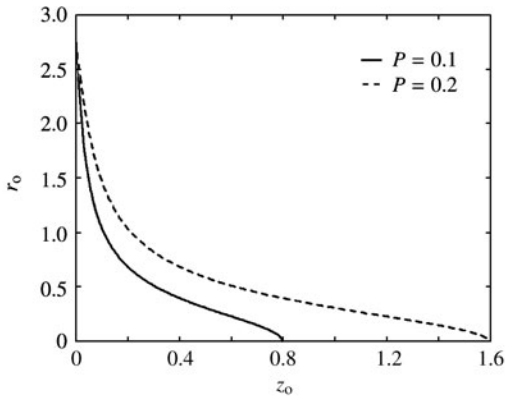

Fig. 11 z_o–r_o relation for a clamped circular plate with $R = 20$ under two different loads of $P = 0.1$ and $P = 0.2$

4 Summary

The differential formulation of the tensionless contact of a finite circular plate presented here offers a more general approach for this type of problem. The matching conditions at the separation point and the solution forms outside the contact area are modified; the plate boundary conditions and the gap distance are incorporated in the formulation. The analysis shows that a plate with a relatively small radius does not lift-off and lifting-off is demonstrated to be dependent on the plate radius and boundary conditions. When the gap distance is zero and the plate radius is large, the contact radius is demonstrated to be independent of the load, which is also shown by previous investigators. For a finite plate with a small radius, the boundary conditions can have significant influence on the contact radius under the same load. However, as the plate radius increases, the contact radius of the plate with zero gap distance becomes insensitive to the boundary conditions and converges to a value close to that of an infinite plate. For the plate with a nonzero gap distance, the contact radius is demonstrated to be dependent on the load, the gap distance, boundary conditions and plate radius.

Appendix

A1. Bessel functions of ber(r), bei(r) and kei (r)

$$\mathrm{ber}(r) = 1 - \frac{(r/2)^4}{(2!)^2} + \frac{(r/2)^8}{(4!)^2} - \frac{(r/2)^{12}}{(6!)^2} + \frac{(r/2)^{16}}{(8!)^2}$$

$$-\frac{(r/2)^{20}}{(10!)^2}+\frac{(r/2)^{24}}{(12!)^2}+\ldots, \tag{A1}$$

$$\begin{aligned}\mathrm{bei}(r)=&\,(r/2)^2-\frac{(r/2)^6}{(3!)^2}+\frac{(r/2)^{10}}{(5!)^2}-\frac{(r/2)^{14}}{(7!)^2}\\&+\frac{(r/2)^{18}}{(9!)^2}-\frac{(r/2)^{22}}{(11!)^2}+\ldots,\end{aligned} \tag{A2}$$

$$\begin{aligned}\mathrm{kei}(r)=&\,(\ln 2-\gamma-\ln r)\mathrm{bei}(r)-\frac{1}{4}\pi\mathrm{ber}(r)+(r/2)^2\\&-\frac{(r/2)^6}{(3!)^2}\left(1+\frac{1}{2}+\frac{1}{3}\right)\\&+\frac{(r/2)^{10}}{(5!)^2}\left(1+\frac{1}{2}+\frac{1}{3}+\frac{1}{4}+\frac{1}{5}\right)\\&-\frac{(r/2)^{14}}{(7!)^2}\left(1+\frac{1}{2}+\frac{1}{3}+\frac{1}{4}+\frac{1}{5}+\frac{1}{6}+\frac{1}{7}\right)+\ldots,\end{aligned} \tag{A3}$$

where $\gamma\approx 0.577\,215\,7$ is the Euler number and $\ln 2-\gamma\approx 0.115\,9$.

A2. Shear force in the lift-off zone of a finite plate

w_2 is the displacement of the lift-off zone, which is an annulus of $r_o\leqslant r\leqslant R$. Substitute w_2 of Eq. (8) into Eq. (10) and after some simple manipulations, the shear force Qr is readily given as follows

$$Q_r(r)=4\frac{C_2}{r},\quad r_o\leqslant r\leqslant R. \tag{A4}$$

For a free circular plate, the boundary condition of zero shear force gives $Q_r(R)=4C_2/R=0$, which yields $C_2=0$. Therefore, $Q_r(r)=0$ in the annulus of $r_o\leqslant r\leqslant R$. For the plate with other type of boundary conditions, $Q_r(R)\neq 0$ and thus $C_2\neq 0$, which is to say that the shear force is not zero in the lift-off zone.

A3. Equation set of A_1, B_1, A_2, B_2, C_2, D_2 and r_o

The four matching conditions of Eqs. (11) and (13) at $r=r_o$ give the following four equations

$$\begin{aligned}&A_1\mathrm{ber}(r_o)+B_1\mathrm{bei}(r_o)-2F_o\mathrm{kei}(r_o)+z_o\\&\quad=A_2r_o^2+B_2\ln r_o+C_2r_o^2\ln r_o+D_2,\end{aligned} \tag{A5}$$

$$\begin{aligned}&A_1\mathrm{ber}'(r_o)+B_1\mathrm{bei}'(r_o)-2F_o\mathrm{kei}'(r_o)\\&\quad=2A_2r_o+\frac{B_2}{r_o}+C_2(2r_o\ln r_o+r_o),\end{aligned} \tag{A6}$$

$$\begin{aligned}&A_1\mathrm{ber}''(r_o)+B_1\mathrm{bei}''(r_o)-2F_o\mathrm{kei}''(r_o)\\&\quad=2A_2-\frac{B_2}{r_o^2}+C_2(2\ln r_o+3),\end{aligned} \tag{A7}$$

$$\begin{aligned}&A_1\mathrm{ber}'''(r_o)+B_1\mathrm{bei}'''(r_o)-2F_o\mathrm{kei}'''(r_o)\\&\quad=2\frac{B_2}{r_o^3}+2\frac{C_2}{r_o},\end{aligned} \tag{A8}$$

here $()'=\mathrm{d}/\mathrm{d}r()$. The displacement constraint condition of Eq. (14) gives the following

$$A_1\mathrm{ber}(r_o)+B_1\mathrm{bei}(r_o)-2F_o\mathrm{kei}(r_o)+z_o=0. \tag{A9}$$

The two boundary conditions for a free plate of Eq. (15) gives the following two equations

$$2A_2(1+\nu)-\frac{B_2}{R^2}(1-\nu)+C_2(2\ln R+1)(1+\nu)+2C_2=0, \tag{A10}$$

$$C_2=0. \tag{A11}$$

There are now seven (nonlinear) equations in total to solve the seven unknowns of A_1, B_1, A_2, B_2, C_2, D_2 and r_o, which can only be done numerically by Newton–Rhapson method. Clearly, Eq. (A10) is the reason why our computed r_o listed in Table 1 is dependent on the plate Poisson's ratio of ν.

The two boundary conditions for a clamped plate of Eq. (16) are the following

$$A_2R^2+B_2\ln R+C_2R^2\ln R+D_2=0, \tag{A12}$$

$$2A_2R+\frac{B_2}{R}+C_2(2R\ln R+R)=0. \tag{A13}$$

References

1 Timoshenko, S., Woinowsky-Krieger, S.: Theory of Plates and Shells (2nd edn), McGraw-Hill Book Company Inc., New York, 1959.

2 Keer, L. M., Dundurs, J., Tsai, K. C.: Problems involving a receding contact between a layer and a half space. J. Appl. Mech. **39**, 1115–1120 (1972)

3 Weitsman, Y.: On the unbonded contact between plates and an elastic half space. J. Appl. Mech. **36**(2), 505–509 (1969)

4 Kerr, A. D.: On the unbonded contact between elastic and elastic-rigid media. Acta Mechanica **33**, 135–146 (1979)

5 Tsai, N. C., Westmann, R. E.: Beams on tensionless foundation. J. Engr. Mech. **93**, 1–12 (1967)

6 Weitsman, Y.: On foundations that reacts in compression only. J. Appl. Mech. **37**(7), 1019–1030 (1970)

7 Celep, Z.: Rectangular plates resting on tensionless elastic foundation. J. Engr. Mech. **114**(12), 2083–2092 (1988)

8 Celep, A., Turhan, D., Al-Zaid, R. Z.: Contact between a circular plate and tensionless edge support. Int. J. Mech. Sci. **30**(10), 733–741 (1988)

9 Silva, A., Silveira. R., Gonclaves, P.: Numerical methods for analysis of plates on tensionless elastic foundations. Int. J. Soilds Struct. **38**, 2083–2100 (2001)

10 Zhang, Y., Murphy, K. D.: Response of a finite beam in contact with a tensionless foundation under symmetric and asymmetric loading. Int. J. Soilds Struct. **41**, 6745–6758 (2004)

11 Zhang, Y.: Tensionless contact of a finite beam resting on Reissner foundation. Int. J. Mech. Sci. **50**, 1035–1041 (2008)

12 Dempsey, J. P., Keer, L. M., Patel, N. B., et al.: Contact between plates and unilateral supports. J. Appl. Mech. **51**, 324–328 (1984)

13 Dempsey, J. P., Li, H.: Rectangular plates on unilateral edge supports: Part1- theory and numerical analysis. J. Appl. Mech. **53**, 146–150 (1986)

14 Zhang, Y.: Extracting nanobelt mechanical properties from nanoindentation. J. Appl. Phys. **107**, 123518 (2010)

15 Zhang, Y., Zhao, Y. P.: Modeling nanowire indentation test with adhesive effect. J. Appl. Mech. **78**, 011007 (2011)

16 Novoselov, K. S., Geim, A. K., Morozov, S. V., et al.: Electric field effect in atomically thin carbon films. Science **306**, 666–669 (2004)

17 Lee, C., Li, Q., Kalb, W., et al.: Frictional characteristics of atomically thin sheets. Science **328**, 76–80 (2010)

18 Carpick, R. W., Agrait, N., Ogletree, D. F., et al.: Variation of the interfacial shear strength and adhesion of a nanometer-sized contact. Langmuir **12**, 3334–3340 (1996)

19 Johnson, K.: Adhesion and friction between a smooth elastic spherical asperity and a plane surface. Proc. Roy. Soc. (London) A **453**, 163–179 (1997)

20 Hu. C., Hartley, G. A.: Analysis of a thin plate on an elastic half-space. Computers & Struct. **52**, 227–235 (1994)

21 Johnson, K. L.: Contact Mechanics, Cambridge University Press, Cambridge, UK, 1985

22 Yang, F.: Contact deformation of a micromechanical structure. J. Micromech. Microengr. **14**, 263–268 (2004)

23 Mastrangelo, C. H., Hsu, C. H.: Mechanical stability and adhesion of microstructures under capillary forces: II. Experiments. J. Microelectromech. Syst. **2**, 44–55 (1993)

24 Zhang, Y., Zhao, Y. P.: Vibration of an adhered microbeam under a periodically shaking electrical force. J. Adhesion Sci. Tech. **19**(9), 799–815 (2005)

25 Zhao, Y. P., Wang, L. S., Yu, T. X.: Mechanics of adhesion in MEMS- a review J. Adhesion Sci. Tech. **17**, 519–546 (2003)

26 Liu, J. L.: Theoretical analysis on capillary adhesion of micro-sized plates with a substrate. Acta Mech. Sin. **26**, 217–223 (2010)

27 Zhang, Y., Zhao, Y. P.: A precise model for the shape of an adhered microcantilever. Sens. Actuators A: Physical **171**, 381–390 (2011)

28 Zhang, Y., Liu, Y., Chen, P., et al.: Nonlinear dynamics response of beam and its application in nanomechanical resonator. Acta Mech. Sin. **28**, 190–200 (2012)

29 McLachlan, N. W.: Bessel Functions for Engineers, (2nd edn), Oxford University Press, London, UK, 1934

30 Hearn, E. J.: Mechanics of Materials, (2nd edn), Pergamon Press, New York, 1985